

## Support Information

### Highly Stretchable, Self-Adhesive, Biocompatible, Conductive Hydrogels as Fully Polymeric Strain Sensors

Dong Zhang<sup>1</sup>, Yijing Tang<sup>1</sup>, Yanxian Zhang<sup>1</sup>, Fengyu Yang<sup>1</sup>, Yonglan Liu<sup>1</sup>, Xiaoyu Wang<sup>2</sup>,  
Jintao Yang<sup>2</sup>, Xiong Gong<sup>3</sup>, and Jie Zheng<sup>1, 3\*</sup>

<sup>1</sup> Department of Chemical, Biomolecular, and Corrosion Engineering  
The University of Akron, Akron, Ohio 44325, USA

<sup>2</sup> College of Materials Science & Engineering  
Zhejiang University of Technology, Hangzhou, 310014, P. R. China

<sup>3</sup> Department of Polymer Engineering  
The University of Akron, Akron, OH 44325, USA

\*Corresponding Author: [zhengj@uakron.edu](mailto:zhengj@uakron.edu)

## Materials and Methods

**Materials.** N-Hydroxyethyl acrylamide (HEAA, >98%) were purchased from TCI Co. Ltd. N-(3-Sulfopropyl)-N-methacryloylamidopropyl-N, N-dimethylammonium betaine (SBAA, 97%) and 2-hydroxy-4'-(2-hydroxyethoxy)-2-methylpropiophenone (Irgacure 2959, 99%) were purchase from Sigma-Aldrich. PEDOT: PSS solution (1.1-1.3% solid content, Clevios HTL Solar) was received from Heraeus Deutschland GmbH & Co. KG. All reagents needed for cell and bacteria assays were described in the corresponding test below. Ultrapure water used in this study was purified by a Millipore water purification system with a resistivity of 18.2 M $\Omega$  cm.

**Fabrication of Conductive poly(HEAA-co-SBAA)/PEDOT: PSS Hydrogels.** Mixture reactants of 3.0 g monomers (HEAA and SBAA (0~26.2 mol%), 3.0 g DI-water, and initiator Irgacure 2959 (1.0 mol% of monomers) were added into beakers. Afterwards, the 0.6 mL pre-whipped PEDOT: PSS aqueous solution (1.1-1.3% solid content) was added into mixture dropwise. After several ultrasonic treatments and fully stirred, the hydrogel precursor was immediately injected into a sealed glass mold with a 1.0 mm thick Teflon spacer and exposed to UV light for 1.5 h (365 nm, 8 W). Note that polymerization time is empirically determined by our preliminary experiments. We found that the longer polymerization times of > 1.5 h lead to very brittle hydrogels due to over-crosslinking effect, while the shorter polymerization times of <1.5 h often suffer from the poor gelation process and in some cases, it cannot even produce hydrogels.

**Tensile Measurements.** As-prepared hydrogels were cut into dumb-bell shape with a width of 3.18 mm, a gauge length of 25 mm, and a thickness of 1.0 mm. Tensile measurements were all performed on a universal tensile machine (Instron 3345, MA) with a 500 N transducer at the stretching rate of 100 mm/min. Here, the tensile strain ( $\epsilon$ ) was defined as the extension distance ( $\Delta L$ ) divided by the initial length ( $L_0$ ).

For hysteresis measurement, hydrogels were first stretched to an extension ratio ( $\lambda=9, 10, \text{ and } 12$ ) and then unloaded. After returning to the original length, the specimens were reloaded and stretched to the same extension ratio ( $\lambda=9, 10, \text{ and } 12$ ) at 100 mm/min. This loading-unloading cycle was repeated four times. Here, dissipated energy was estimated by area below the stress-strain curves or between the loading-unloading curves. As for successive loading-unloading measurements, the loading-unloading operations were repeatedly conducted on the same specimen with increasing extension ratios ( $\lambda=3, 6, 9, \text{ and } 12$  gradually) until the sample failed at an elongation break.

**FTIR-ATR Spectral Analysis.** Fourier-transform infrared spectroscopic (FT-IR) analysis was recorded by using a Thermo Nicolet (Nicolet 6700) with resolution at 4 cm<sup>-1</sup> and scans at 32, which completely evaluated chemical structures of lyophilized hydrogels. 2D FTIR spectra were processed by Software (2Dshige version 1.3) based on a series of in-situ FTIR spectra of hydrogels as temperatures increased from 25 °C to 50 °C.

**Zeta Potential.** Since bulk hydrogel samples cannot directly be used for Zeta potential test, we fabricated microgels and tiny fragments of bulk hydrogels by using same feed ratios of monomers and initiators. The measurements of zeta potential was conducted using a NanoBrook Omni Particle Size and Zeta Potential analyzer (Brookhaven Instruments, NY) at room temperature. The pH value of sample solution was adjusted to 1~2 for eliminating the influence of the acidic solvent inside hydrogel on the actual potential.

**Electrochemical Performance Measurement.** Conductivity of each tested hydrogel (cylindrical, diameter of 1.35 cm) was firstly measured by four-probe AC impedance spectrum. Then initial electrical resistance of hydrogel sample  $R_0$  ( $\Omega$ ) was calculated according to the following equation.

$$R_0 = \frac{d}{S \times \delta}$$

*Note:* where  $d$  (cm) is the distance between two probes,  $\delta$  is the conductivity of hydrogel and  $S$  (cm<sup>2</sup>) is cross-sectional area of tested hydrogel.

Resistance change was further recorded by using classic electrochemical workstation (Princeton Applied Research VERSAST3-200, USA). Generally, hydrogel samples were equipped to corresponding Mode (self-adhesive/stretching-sensitive and pressure-sensitive mode, see Figure 4a) and connected with test electrochemical workstation. To prevent moisture evaporation, the equipped sensors can be attached with VHB tape. Relative resistance change of the hydrogel samples was determined as following equations.

$$\frac{\Delta R}{R_0} = \frac{R_r - R_0}{R_0} \times 100\%$$

*Note:* where  $R_r$  denotes the real-time resistance and  $R_0$  belongs to the resistance without any strain here.

EIS (Electrochemical impedance) measurement was performed with the frequency ranging from 10 mHz to 100 kHz and an impedance amplitude of  $\pm 5$  mV at open circuit potential by using a Gamry Reference 3000 electrochemical workstation (Gamry Instruments, USA).

**Peeling Test.** Briefly, all non-porous solid substrates, i.e. glass, ceramic, aluminum sheet, and titanium sheet were sequentially cleaned with 30-min sonication in ethanol, acetone, and water and completely dried (beef tissue was applied for preparation directly after drying the superficial water). Afterwards, the cleaned and dried substrates were directly used as molds without any further treatment. For easier de-molding, a clean PET film was used to cover one side of the mold, which was similar with previously reported<sup>1</sup>. The following process was the same as the normal hydrogel synthesis procedure as stated above. To obtain various thickness of hydrogel sheet on substrate, Teflon spacers (thickness: 3 mm) were used. Practical 90° peeling tests were performed by a universal tensile machine (Instron 3345, MA) equipped peeling fixture (Mecmesin, ACC008-208) with a speed of 50 mm/min. As a stiff backing for the hydrogel sheet during the test, the Scotch duct tape (3M) were adhered on the top of hydrogel via super-glue. Interfacial toughness ( $T_I$ ) were estimated by following equation.

$$T_I = \frac{F_{ave}}{w}$$

*Note:* where  $F_{ave}$  is the average force at the plateau in the steady-state region of peeling process, for those gels did not reach the steady state, the force at the fracture point was used;  $w$  is the width of tested hydrogel sheet.

**Cell Assay.** Bovine aortic endothelial cells (BAEC) were chosen to challenge the hydrogel samples. Note that all disk-like hydrogels need to soak into PBS solution thoroughly for 3 days in order to remove unreacted monomers and make sure the hydrogel samples are sterile. Briefly, BAEC cell lines were firstly culture in the special-made DMEM-based medium on a tissue culture polystyrene flask for ~72 h to reach a high density. Then, BAEC were removed from the flask by the reported protocol and diluted to a concentration of  $10^5$  cells·mL<sup>-1</sup>. Then a diluted 3 mL cell suspension was added to each corresponding well after hydrogel samples were placed into a six-well plate. The incubated temperature was controlled at 37 °C for another 72 h. Cell morphology were determined by an EVOS XL core inverted microscope with a 10× objective.

*Note:* For better distinguishing the BAEC cells, we stained the cells in green color since initial images were all gray (More detailed information see Figure 6).

**MTT Cell Toxicity Assay.** Before applying hydrogels to any cell assay, the hydrogels were

exposed to UV light for 10 min for sterilization. To determine the cell viability, colorimetric MTT metabolic activity assay was performed. Briefly, SH-SY5Y cells with a concentration of  $10^4$  cells/mL were cultured in a 96-well plate at 37 °C. Then, six disk-like pure PHEAA hydrogels and conductive poly(HEAA-*co*-SBAA)/PEDOT: PSS hydrogels were individually added to each well, which were then continually cultured for additional 24 h (or 48 h). After removing the supernatant and hydrogel samples of each well, 20  $\mu$ L of MTT solution (5 mg/mL in PBS) and 100  $\mu$ L medium were then added into the systems. Formazan-dimethyl sulfoxide solution (150  $\mu$ L) was then added and the absorbance intensity was measured using a micro-plate reader (Bio-RAD 680, USA) at 570 nm after another 4 h incubation. Note that the relative cell viability (%) was normalized by the percentage relative to the untreated control cells.

**LDH Cytotoxicity Assay.** It was assessed using the LDH assay kit (Thermo, USA) according to the manufacturer's instructions. Briefly, SH-SY5Y cells with a concentration of  $10^4$  cells/mL were cultured in a 96-well plate at 37 °C. Then, six disk-like sterile pure PHEAA hydrogels and conductive poly(HEAA-*co*-SBAA)/PEDOT: PSS hydrogels were individually added to each well, which were then continually cultured for additional 24 h (or 48 h). Afterwards, 10  $\mu$ L of Lysis Buffer was added to the wells containing untreated control cells prior to the assay to induce maximum LDH release. After incubation for 45 min, 50  $\mu$ L supernatant from each well (including untreated control, treated and maximum LDH release groups) was transferred to a new 96-well plate (Mark position). Subsequently, 50  $\mu$ L of the reaction mixture was added to each sample well and incubated at room temperature for 30 minutes in the dark place. Stop solution (50  $\mu$ L) was added to each well and the absorbance was measured using a micro-plate reader (Bio-RAD 680, USA) at the wavelengths of 490/680 nm.

**Bacterial Assay.** *E. coli* (Gram-negative) and *S. epidermidis* (Gram-positive) were chosen for the bacterial attachment assay. Note that all disk-like hydrogels need to soak into PBS solution thoroughly for 3 days in order to remove unreacted monomers and make sure the hydrogel samples are sterile. Specifically, several colonies of each bacteria were firstly chosen and incubated in moderate LB medium to get the initial bacterial culture solutions. Then the initial bacterial solution were diluted to a density of  $10^5$  cells/cm<sup>2</sup>. Then the diluted 4 mL bacterial suspension was added to each well after sterilized disk-like hydrogels were placed into a six-well plate. Whole system was incubated under 37 °C for ~12 h, afterwards, the samples were washed with Millipore water twice, subsequently stained with a Live/Dead BacLight kit (Thermo Fisher Scientific Inc., NY) before imaging. Bacterial morphology was then measured by the Olympus IX81 fluorescence microscope with a 40 $\times$  lens.

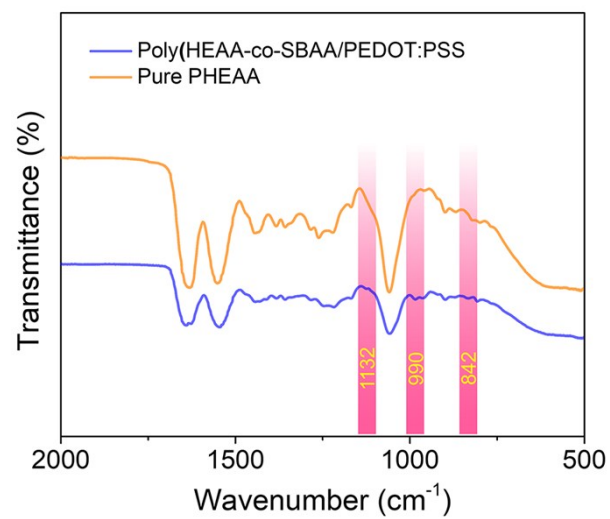


**Figure S1.** FTIR-ATR spectra of freeze-dried poly(HEAA-co-SBAA)/PEDOT: PSS hydrogel (SBAA: 9.8 mol%) and pure PHEAA hydrogel.

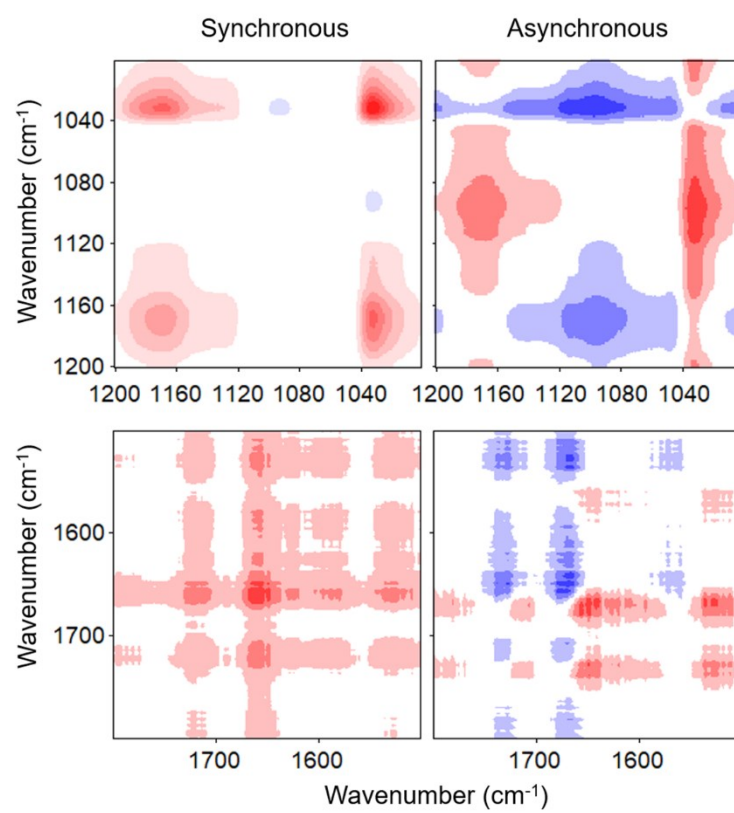


**Figure S2.** 2D-FTIR synchronous and asynchronous spectra of poly(HEAA-co-SBAA)/PEDOT:PSS hydrogel.

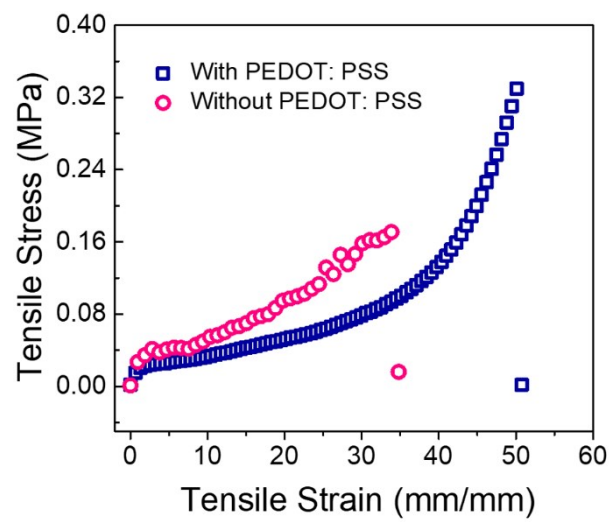


**Figure S3.** Comparison of tensile properties between poly(HEAA-*co*-SBAA) hydrogels with and without PEDOT: PSS.

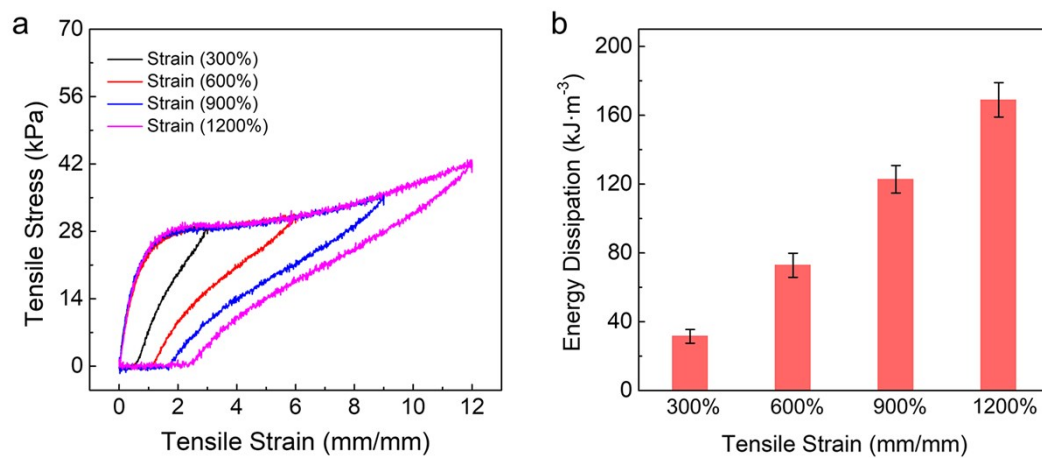


**Figure S4.** (a) Cyclic loading-unloading and (b) Energy dissipation of poly(HEAA-co-SBAA)/PEDOT: PSS hydrogel at different tensile strains.

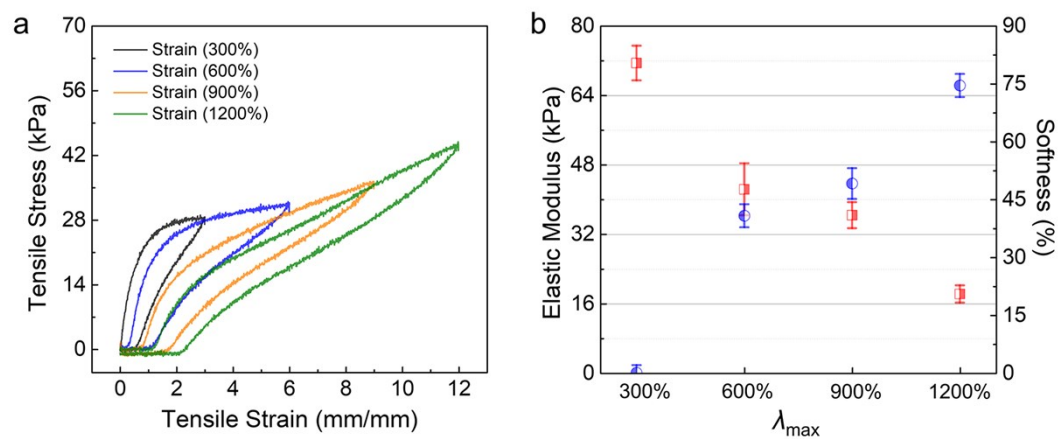


**Figure S5.** (a) Successive loading–unloading curves and (b) Statistics of elastic modulus and softness of the same of poly(HEAA-*co*-SBAA)/PEDOT: PSS hydrogel at different  $\lambda_{\max}$  of tensile strains. No resting time is applied between any two consecutive loadings.

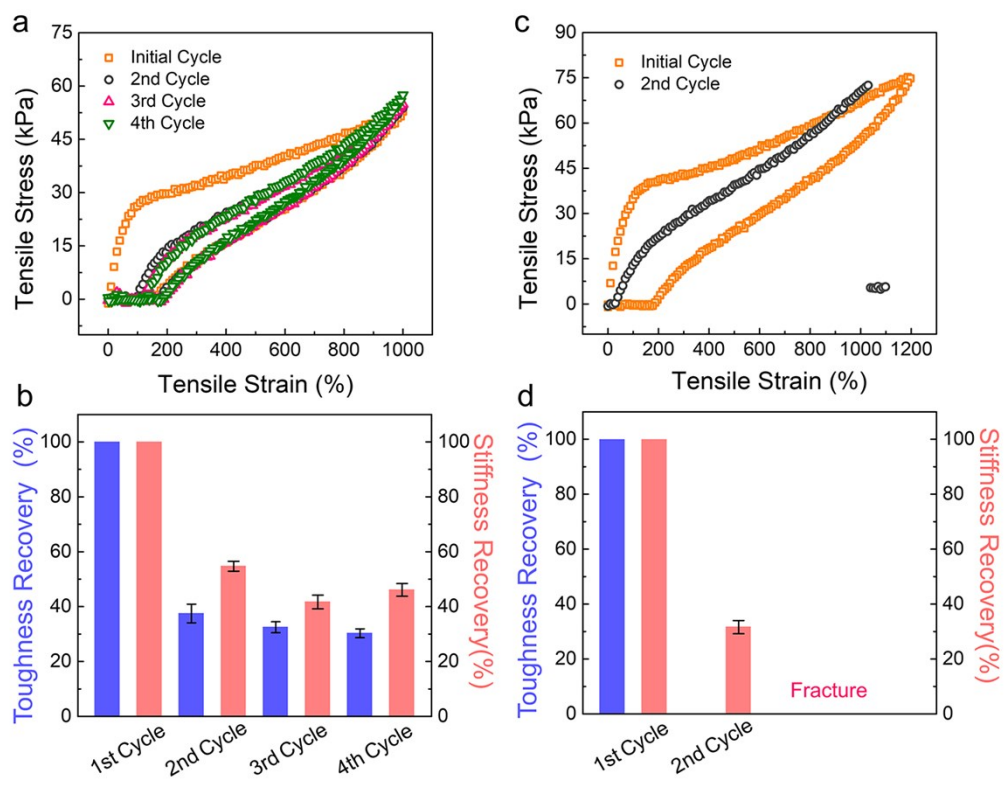


**Figure S6.** (a, c) Cyclic loading-unloading curves and (b, d) the corresponding toughness/stiffness recovery of poly(HEAA-co-SBAA)/PEDOT:PSS hydrogels at a strain of (a, b) 1000% and (c, d) 1200%.

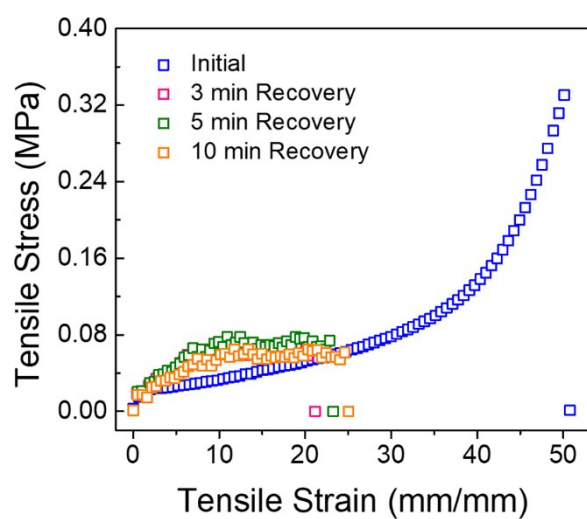


**Figure S7.** Mechanical recovery of self-healed poly(HEAA-*co*-SBAA)/PEDOT: PSS hydrogel after 3 , 5 , and 10 min self-healing at room temperature.

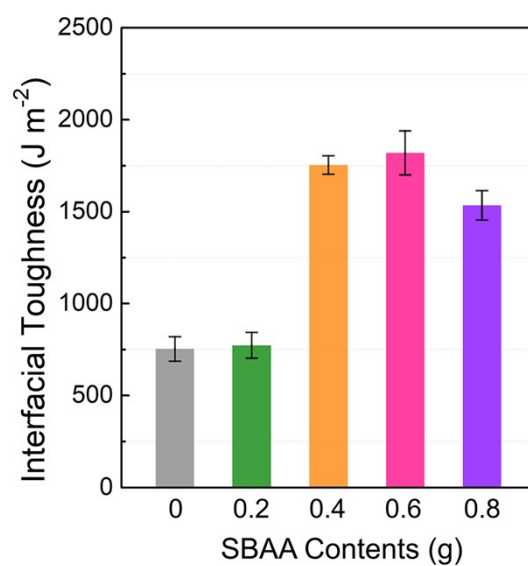


**Figure S8.** Peeling interfacial toughness of poly(HEAA-*co*-SBAA)/PEDOT: PSS hydrogels prepared with different SBAA contents (0~0.8 g) on nonporous glass at a peeling rate of 50 mm/min.

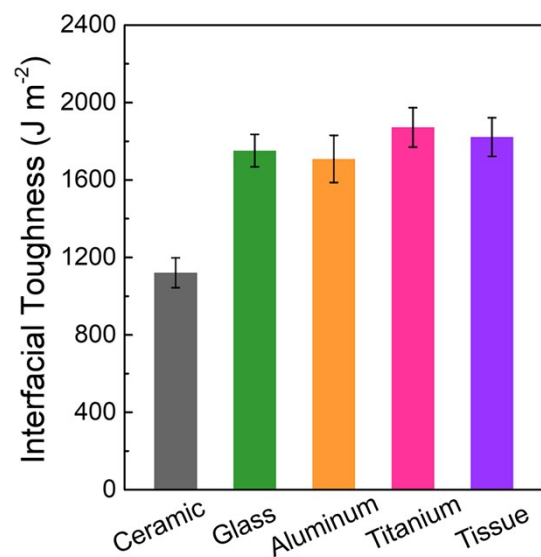


**Figure S9.** Interfacial toughness of poly(HEAA-co-SBAA)/PEDOT:PSS hydrogels on ceramic, glass, aluminum, titanium, and beef tissue substrates at a peeling rate of 50 mm/min.

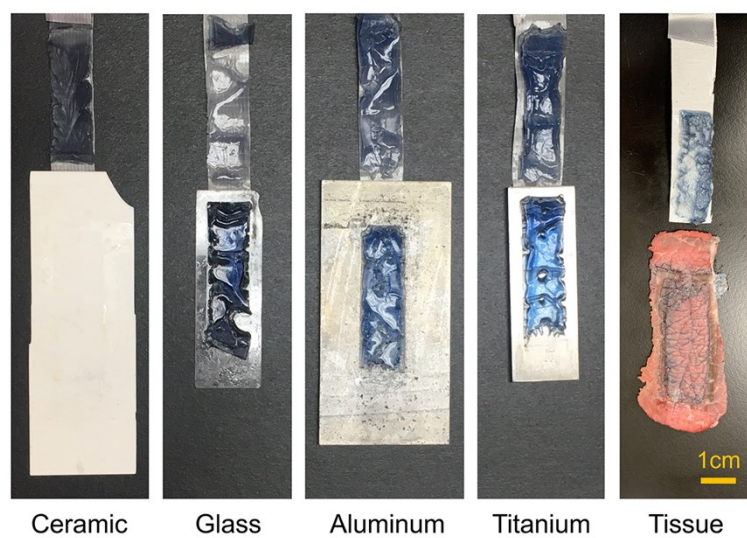


**Figure S10.** Hydrogel residues left on ceramic, glass, aluminum, titanium, and beef tissue substrates after peeling poly(HEAA-co-SBAA)/PEDOT: PSS hydrogels off from these surfaces.

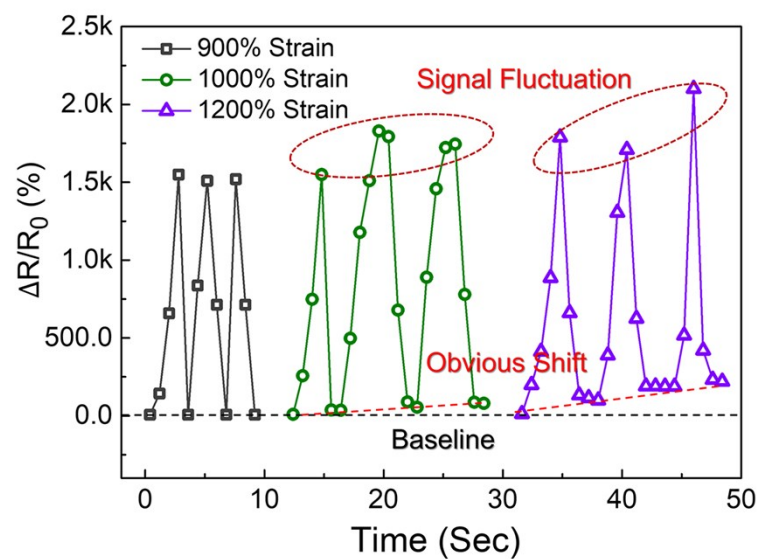


**Figure S11.** Relative resistance changes of poly(HEAA-co-SBAA)/PEDOT:PSS hydrogel sensors in response to repeatable stretching/releasing motions at different strains of 900%, 1000%, and 1200%.

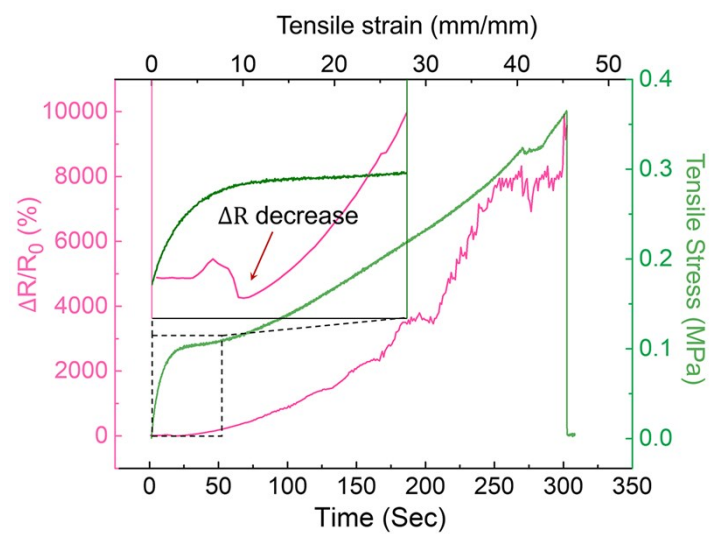


**Figure S12.** Strain-induced tensile stress and current sensing curves of poly(HEAA-co-SBAA)/PEDOT:PSS hydrogel sensor.

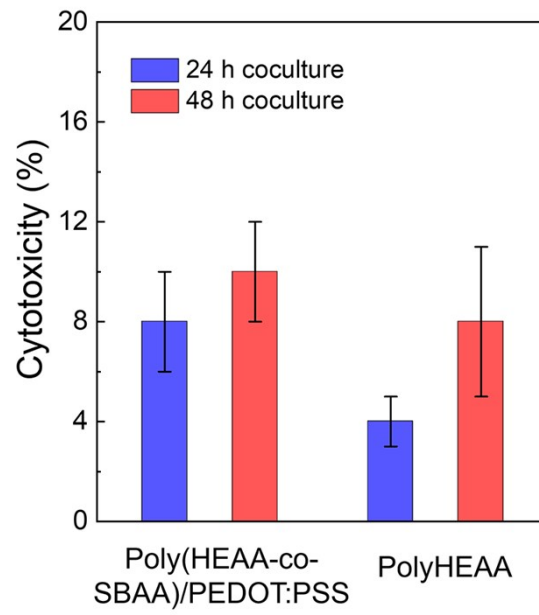


**Figure S13.** LDH assay to show cell cytotoxicity as induced by pure polyHEAA and poly(HEAA-co-SBAA)/PEDOT: PSS hydrogels after 24 h and 48 h incubation of SH-SY5Y cells.

**Table S1.** Zeta potential of as-reprepared poly(HEAA-co-SBAA)/PEDOT: PSS microgel and tiny fragment solution. (pH=1~2)

Sample	Zeta Potential (mV)
Microgel (Solution)	1.08±0.3
Tiny fragment (solution)	-0.66±0.5

**Table S2.** A summary and comparison of poly(HEAA-*co*-SBAA)/PEDOT: PSS sensor with other polymeric hydrogel-based strain sensors in terms of gauge factor, stretchability, and sensing properties.

Hydrogel Sensors	Signal	GF	Stretchability	Sensing Properties
PANI-poly(AAm- <i>co</i> -HEMA) <sup>2</sup>	Electric	GF=11	~300%	Detect wrist bending, speaking; biocompatible
PANI/PSS-UPyMA <sup>3</sup>	Electric	GF=3.4	~300%	Self-healing (<30 s); detect pulse beating, speaking, finger bending
polyNIPAAm/PANI <sup>4</sup>	Electric	GF=3.92	~200%	Stable performance (~350 cycles)
PIL-BF <sub>4</sub> /PEDGA <sup>5</sup>	Electric	GF=~1.5	>1400%	Wide working condition (-75°C to 340°C); detect finger bending (>10000 fatigue cycles)
TA/sodium alginate (SA)-polyAAm <sup>6</sup>	Electric	GF=2.0	>2100%	Self-healing; detect smiling, finger bending, and wrist pulse
NaCl-gelatin/PVA <sup>7</sup>	Electric	GF=~0.4	~715%	Lower working condition (-20°C); detect finger and elbow bending, speaking
LiCl-polyAAm <sup>8</sup>	Capacitance	GF=~1.3	>1000%	Detect location of touch (work as smart screen)
NaCl-SA/ polyAAm <sup>9</sup>	Electric	GF=2.0	~3120%	Detect speaking, finger bending, and wrist pulse
PVA/RSF/borax <sup>10</sup>	Electric	GF=~0.7	~5000%	Track leg, knee bending and different gestures
PDA/polyAAm <sup>11</sup>	Electric	GF=~1.0	~700%	Self-adhesive; wide working condition (-20~60°C); detect arm bending and wrist pulse
NaCl-polyAAm <sup>12</sup>	Capacitance	GF=~1.0	>590%	Detect finger bending (>4000 cycles) and location of touch
This work	Electric	GF=~2.0	~5000%	Self-healing (<3 min); Detect compression, speaking, and finger/leg bending with varying degree

## References

1. H. Chen, Y. Liu, B. Ren, Y. Zhang, J. Ma, L. Xu, Q. Chen and J. Zheng, *Adv. Func. Mater.*, 2017, **27**, 1703086.
2. Z. Wang, J. Chen, Y. Cong, H. Zhang, T. Xu, L. Nie and J. Fu, *Chem. Mater.*, 2018, **30**, 8062-8069.
3. J. Chen, Q. Peng, T. Thundat and H. Zeng, *Chem. Mater.*, 2019, **31**, 4553-4563.
4. Z. Wang, H. Zhou, W. Chen, Q. Li, B. Yan, X. Jin, A. Ma, H. Liu and W. Zhao, *ACS Appl. Mater. Interfaces*, 2018, **10**, 14045-14054.
5. Y. Ren, J. Guo, Z. Liu, Z. Sun, Y. Wu, L. Liu and F. Yan, *Sci. Adv.*, 2019, **5**, 1-10.
6. H. Qiao, P. Qi, X. Zhang, L. Wang, Y. Tan, Z. Luan, Y. Xia, Y. Li and K. Sui, *ACS Appl. Mater. Interfaces*, 2019, **11**, 7755-7763.
7. H. Chen, X. Ren and G. Gao, *ACS Appl. Mater. Interfaces*, 2019, **11**, 28336-28344.
8. Chong-Chan Kim, Hyun-Hee Lee, Kyu Hwan Oh and J.-Y. Sun, *Science*, 2016, **353**, 682-687.
9. X. Zhang, N. Sheng, L. Wang, Y. Tan, C. Liu, Y. Xia, Z. Nie and K. Sui, *Mater Horiz*, 2019, **6**, 326-333.
10. N. Yang, P. Qi, J. Ren, H. Yu, S. Liu, J. Li, W. Chen, D. L. Kaplan and S. Ling, *ACS Appl. Mater. Interfaces*, 2019, **11**, 23632-23638.
11. L. Han, K. Liu, M. Wang, K. Wang, L. Fang, H. Chen, J. Zhou and X. Lu, *Adv. Func. Mater.*, 2018, **28**, 1704195.
12. J. Y. Sun, C. Keplinger, G. M. Whitesides and Z. Suo, *Adv. Mater.*, 2014, **26**, 7608-7614.